Biophysical Journal Volume 89 September 2005 1978–1983

Effects of Urea and Trimethylamine-*N*-Oxide (TMAO) on the Interactions of Lysozyme in Solution

Marc Niebuhr and Michel H. J. Koch
European Molecular Biology Laboratory, Hamburg Outstation, D-22603 Hamburg, Germany

ABSTRACT The effect of two physiological cosolutes (urea and trimethylamine-*N*-oxide) and of KCl on the intermolecular interactions in concentrated lysozyme solutions were studied by synchrotron radiation small angle x-ray scattering. The evolution of the structure factors as a function of cosolute and/or salt concentration was modeled using pair potentials following an approach recently described in the literature. It was found that the structure factors for salt and/or cosolute concentration series at a fixed protein concentration can best be described using a variable depth attractive potential and a constant effective charge rather than a constant attractive potential and a variable effective charge as done in previous work.

INTRODUCTION

Intermolecular forces play a central role in the properties of biological macromolecules in solution as well as in vivo. In vivo, different contributions to these forces (e.g., electrostatic, hydrophobic, hydration, etc.) (1) are modulated among others by the presence of cosolutes—mainly salts and small molecules. The physiological importance of cosolutes like urea and trimethylamine-*N*-oxide (TMAO), which are present in large concentrations in the intracellular fluids of many species of all kingdoms and in particular in marine animals, has been extensively documented (see, e.g., Hochachka and Somero (2)).

In vitro, the interactions between macromolecules result in nonideality of solution properties and influence osmotic pressure, solubility, crystallization, and/or precipitation. In recent years many aspects of the interactions of—mainly globular—proteins in solution have been successfully studied by osmotic pressure measurements and light or x-ray scattering methods. This has given new insights into important physiological phenomena like the transparency of the eye lens (for a review, see Bloemendal et al. (3)).

The small angle x-ray scattering pattern of moderately concentrated monodisperse protein solutions can be represented as the product of the form factor (FF(s)), which is determined by the shape of the individual proteins, and a concentration (c) dependent structure factor (SF(s)), which reflects the structure of the solution and the intermolecular interactions and is directly related to the osmotic pressure (for an introduction, see, e.g., Koch et al. (4)).

$$I(c,s)/c \quad = \mathrm{FF}(s) \times \mathrm{SF}(c,s). \qquad (1)$$

Both form and structure factors are functions of the modulus of the momentum transfer vector ($s = 4\pi \sin\theta/\lambda$, where 2θ is the scattering angle and λ the wavelength of the incident radiation) and may also depend on other factors like temperature, pH, and cosolute concentration.

Extensions of models initially developed for calculating the structure factors of simple liquids have been successfully used to model the effect of pH, temperature, salts, or polyethylene glycol on the interactions of proteins in solution with the aim of laying the foundations for rational crystallization methods (5–7). In contrast the effects of physiological cosolutes on these interactions and their modeling seem to have hitherto received relatively less attention (8–10).

Below we report the results of an investigation of the effects of urea and TMAO on the salt dependence of the interactions in lysozyme solutions. The choice of this system is based on the fact that as the interactions of lysozyme in solution have been investigated in some detail both experimentally and theoretically (6), it provides a natural benchmark for further studies.

The results confirm that, as previously observed (6), the effects of salt on the structure factors of concentrated protein solutions in deionized water can satisfactorily be explained using a pair potential with a constant attractive term and a variable effective charge. This also applies to solutions containing 250 mM urea but not to solutions containing 250 mM TMAO. In this case a variable attractive potential is indispensable to model the observations. The use of a variable attractive potential and a fixed effective charge also yields a better fit to the experimental data for lysozyme solutions in deionized water or 250 mM urea.

MATERIALS AND METHODS

Sample preparation

Lyophilized lysozyme powder (95% protein, Sigma-Aldrich, Taufkirchen, Germany) was resuspended in a small amount of deionized water and dialyzed at room temperature under continuous stirring in three steps of typically 1, 2, and 10 h, against 200–1000 ml deionized water using dialysis cassettes

Submitted April 1, 2005, and accepted for publication May 31, 2005.

Address reprint requests to Michel H. J. Koch, Tel.: 49-40-89902-113; Fax: 49-40-89902-149; E-mail:koch@embl-hamburg.de.

Marc Niebuhr's present address is Stanford Synchrotron Radiation Laboratory, Stanford Linear Accelerator Center, MS69, 2575 Sand Hill Road, Menlo Park, CA 94025.

0006-3495/05/09/1978/06 $2.00

doi: 10.1529/biophysj.105.063859

(Slide-A-Lyzer; Extra Strength; 10,000 MWCO, Pierce, Rockford, IL). With typical cassette volumes between 0.5 and 3 ml, dilution factors between 60 and 2000 per step were achieved. Before dialysis the samples were homogenized by vortexing. After dialysis undissolved material was removed from the sample by centrifugation (5415 C, Eppendorf, Hamburg, Germany) for 15 min at maximum speed (14,000 rpm; 12,500 *g*).

The samples for the salt series were prepared by mixing appropriate volumes of stock solutions of lysozyme (91 mg/ml), KCl (2 M), and urea (2 M, purity >99.5%, Carl Roth GmbH, Karlsruhe, Germany) or TMAO dihydrate (2 M, purity >99%, Sigma-Aldrich) to obtain the required final concentrations. The KCl target concentrations were 0, 5, 10, 20, 50, 100, and 250 mM, those of urea or TMAO 250 mM. The final lysozyme concentration was 68 mg/ml for all salt series. The pH of the solutions in deionized water varied between 6.5 and 7 and was ~7 in the presence of urea and ~8 in the presence of TMAO. After mixing, the samples were vortexed for ~10 s.

A series with TMAO concentrations (0, 10, 20, 50, 100, 250, 500, 750, 1000 mM) in deionized water with 45.5 mg/ml lysozyme was prepared as described above. For the determination of the form factor, samples with a lower lysozyme concentration (6.8 mg/ml) in deionized water or 250 mM TMAO were used.

Protein concentrations were determined by absorbance measurements at 280 nm in a Uvikon 922 (Kontron, Munich, Germany) or an Ultrospec 3000 (GE Healthcare, Munich, Germany) spectrophotometer assuming an absorbance of 2.46 for 1 mg/ml lysozyme in a 1 cm cuvette at 280 nm.

X-ray measurements

X-ray solution scattering patterns were recorded on the X33 beam line (11) of the European Molecular Biology Laboratory on the storage ring DORIS of the Deutsches Elektronen Synchrotron (DESY) using a linear position sensitive gas proportional detector with delay line readout (12). The patterns covered the range of momentum transfer $0.018\ \text{Å}^{-1} \le s \le 0.3\ \text{Å}^{-1}$, where $s = 4\pi\sin\theta/\lambda$, 2θ is the scattering angle, and λ the wavelength of the incident radiation (0.15 nm).

The patterns were recorded in 10 or 15 1-min frames depending on protein concentration to monitor possible radiation damage. Buffer patterns were recorded before and after each protein pattern. The final scattering patterns were obtained after averaging the frames that were statistically identical, correction for detector response, normalization to the intensity of the transmitted beam and the protein concentration, and subtraction of an averaged buffer pattern using the program SAPOKO (13). The patterns were scaled in the range $0.188\ \text{Å}^{-1} \le s \le 0.215\ \text{Å}^{-1}$ to correct for small differences in concentration and contrast.

Data analysis

Ideally, the form factor is determined by extrapolation of a series of scattering patterns at different concentrations to infinite dilution. In the case here, the patterns of a dilute solution (6.8 mg/ml) in deionized water or in 250 mM TMAO and a concentrated solution (68 mg/ml) of lysozyme in the same solvent were spliced in the range $0.160\ \text{Å}^{-1} \le s \le 0.215\ \text{Å}^{-1}$ and used to determine the form factor with the program GNOM (14). Data points for $s < 0.05\text{Å}^{-1}$ which were clearly affected by intermolecular interactions were excluded from the fit. This form factor, obtained as the inverse transform of the distance distribution function $p(r)$, was identical to that obtained from a similar lysozyme solution in 50 mM sodium acetate, pH 4.5. The structure factors of the different solutions were obtained by dividing their scattering pattern by this smooth form factor to avoid the propagation of statistical fluctuations in the pattern of the dilute solution to the structure factors measured at high concentrations.

Further analysis was based on an approach which was successfully used in the description of interactions of proteins in solutions (6). This approach relies on models of the pair potential allowing the calculation of the pair distribution function $g(r)$, which for a solution with number density of particles ρ is directly related to the structure factor by Eq. 2:

$$\mathrm{SF}(c,s) = 1 + \rho \int_0^\infty 4\pi r^2 (g(r) - 1)\sin(rs)/(rs)\ \mathrm{d}r. \quad (2)$$

The model of the pair potential derived from the DLVO (Derjaguin, Landau, Verwey, Overbeek) theory (15) is based on three types of interactions. The first type is represented by a hard sphere potential (diameter σ), reflecting the fact that proteins do not interpenetrate. Long-range electrostatic interactions and various short-range attractive interactions (such as hydrogen bridges, hydrophobic forces, and van der Waals forces) are represented by two Yukawa potentials, one attractive the other one repulsive. The effective pair potential thus becomes

$$u(\vec{r}) = \begin{cases} \infty & \text{if} \quad r \le \sigma \\ J_\mathrm{a}\,\sigma/r \exp(-(r-\sigma)/d_\mathrm{a}) & \\ \quad + J_\mathrm{r}\,\sigma/r \exp(-(r-\sigma)/d_\mathrm{r}) & \text{if} \quad r > \sigma \end{cases}. \quad (3)$$

J_a, d_a are the depth (in units of kT) and range of the attractive potential and J_r, d_r those of the repulsive potential. In the DLVO theory J_r, d_r are functions of the effective number of charges on the protein (Z_p) and the Debye length (λ_D), which is itself a function of the ionic strength. For monovalent salts like NaCl, $\lambda_\mathrm{D} = 3.04/[\mathrm{NaCl}]^{1/2}$ Å at 25°C (1), where the decrease of this range parameter with increasing salt concentration reflects charge screening.

The depth of the repulsive potential $J_\mathrm{r} = \left(Z_\mathrm{P}^2/\sigma\right) \times \left(L_\mathrm{B}/(1+\sigma/2\lambda_\mathrm{D})^2\right)$, where $L_\mathrm{B} = e^2/4\pi\varepsilon_0\varepsilon_\mathrm{s}kT$ is the Bjerrum length of the solvent, which has a value of 7.2 Å at 300 K, e is the elementary charge, ε_0 the permittivity of vacuum, ε_s the relative permittivity, k the Boltzmann constant, and T the absolute temperature. As the value of the relative permittivity of urea and TMAO solutions for concentrations below 1 M are only slightly higher (~2%) than that of pure water (16,17), this value was kept constant in the calculations.

The parameters of the attractive potential (J_a, d_a) are best determined in the attractive regime, which is most easily reached by addition of salt.

The hypernetted chain approximation relating the pair distribution function ($g(r)$) to the total ($h(r) = g(r) - 1$) and direct $c(r)$ correlation functions (Eq. 4) was used to solve the Ornstein-Zernicke relation numerically (6). For this purpose, a computer program was written to model the structure factors from the pair potentials, using an iterative algorithm similar to that of Belloni (18):

$$g(r) = exp[-u(r)/k_\mathrm{B}T + h(r) - c(r)]. \quad (4)$$

RESULTS AND DISCUSSION

The scattering patterns of the 6.8 mg/ml lysozyme solutions in deionized water and in 250 mM TMAO were identical above $s = 0.05\ \text{Å}^{-1}$, as illustrated in Fig. 1. These individual curves as well as the complete form factor yielded a maximum particle dimension $D_\mathrm{max} = 46$ Å and a radius of gyration of $R_\mathrm{g} = 15.4 \pm 0.2$ Å. These values are in good agreement with previous experimental data for monodisperse solutions of lysozyme (see, e.g., Svergun et al. (19)) and with those calculated from the crystallographic model of lysozyme (20) (entry 193L in the Protein Data Bank (21)) with the program CRYSOL (22)).

The intensity scattered at small angles is dominated by the contribution of the shape scattering and is thus proportional to the square of the contrast between protein and solvent (i.e., the total excess scattering length density $\bar{\rho}$) and to the concentration. The electron density of proteins is typically $\sim 0.42\ \text{Å}^{-3}$, whereas that of the solvent depends on the salt

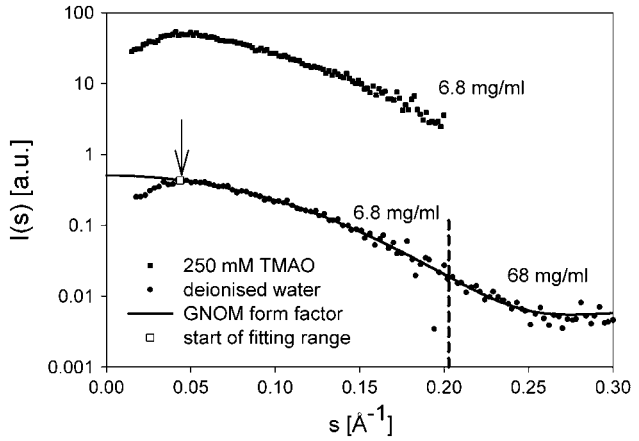

FIGURE 1 Scattering pattern of a lysozyme solution (6.8 mg/ml) in deionized water (*bottom*) and 250 mM TMAO (*top*). The form factor was calculated from the pattern in water spliced with that of a concentrated solution (68 mg/ml) at $s = 0.215$ Å^{-1}, as indicated by the vertical dashed line. Data points for $s < 0.05$ Å^{-1} affected by intermolecular interactions were not included in the GNOM fit.

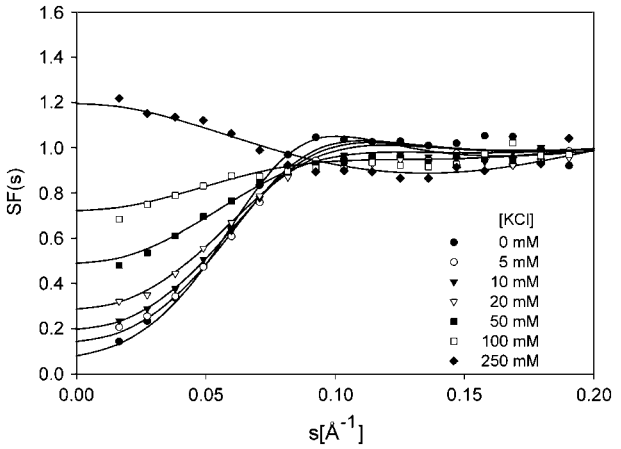

FIGURE 2 Experimental and calculated (*thick lines*) structure factors for lysozyme solutions (68 mg/ml) with different KCl concentrations. For clarity, only 1 experimental point in 20 is displayed.

and cosolute concentration. It increases from 0.334 Å^{-3} in pure water to 0.337 Å^{-3} in a 250 mM KCl solution. The ensuing drop in contrast of ~3% from 0.086 Å^{-3} to 0.083 Å^{-3} results in a reduction in the scattered intensities of ~7%. These differences were corrected together with small differences in protein concentration due to mixing by normalizing the scattering curves in the range 0.188 Å$^{-1} \leq s \leq 0.215$ Å^{-1}. As all curves are superimposable on a logarithmic scale in this range, it can be assumed that the interactions no longer influence the scattering pattern. This procedure, which effectively forces the average value of the structure factor in this interval to 1, was applied to all series discussed in the following section.

The structure factors for the KCl concentration series in water for a lysozyme concentration of 68 mg/ml are shown in Fig. 2. The first question arising during the selection of the fitting parameters concerns the choice of the Debye length. Total absence of ions would require an infinite Debye length and correspond to an infinite repulsive potential in the DLVO theory, but even after extensive dialysis against deionized water a small amount of ions including H_3O^+ and OH^- remains in solution. In the case here, a Debye length of 26.3 Å, corresponding to an effective monovalent ion concentration of 13 mM, fits the data in deionized water. This inherent ionic concentration was also taken into account in the calculation of the Debye length for the KCl concentration series in Table 1.

An effective number of charges of 6.5 yields the best fit to the experimental data. In the case of deionized water, the value of the hard sphere diameter σ has little influence on the shape of the curves, and a value of 28.4 Å was chosen based on the fits to the measurements at higher salt concentrations. For the Yukawa potential a value of 3.0 Å, representing a realistic short-range attractive potential (6), was used to facilitate comparison with previous results. The depth of the attractive potential, which decreases from −5.3 kT at 0 mM KCl to −3.5 kT at 250 mM KCl and 20°C was varied to fit the individual curves, and the final values for the different KCl concentrations are given in Table 1. The value of the effective charge is compatible with hydrogen ion titration (23) on lysozyme solutions of 7–12 mg/ml at pH 7, which yields a nearly constant value of $Z_p = 7$ in the range of KCl ionic strength between 0.1 and 0.2 M.

Fig. 3 presents the statistical errors on the structure factors calculated from the experimental data assuming a 1% relative error on the form factor based on the fact that the errors on $I(0)$ and R_g in the GNOM fit were of the order of 0.5%. The plot illustrates that there are systematic deviations between model and measurements, especially in the attractive regime. This is not surprising given the simplifying assumption of the model (e.g., spherical shape of the protein).

In the case here, it is possible to find an attractive potential with a constant depth (−2.84 kT at 20°C) and range (3.0 Å) which satisfactorily fits all curves with an effective charge of

TABLE 1 Values of the Debye length (λ_D), taking into account the inherent monovalent ion concentration of 13 mM for different KCl concentrations and depth of the repulsive (J_r) and attractive (J_a) potentials (in kT at 20°C) yielding the best fit to the experimental structure factors

KCl [mM]	λ_D (Å)	J_r	J_a (deionized water)	J_a (urea 250 mM)	J_a (TMAO 250 mM)
0	26.3	2.5	−5.3 ± 0.5	−3.7 ± 0.5	−6.9 ± 0.5
5	22.4	2.1	−4.1 ± 0.5	−3.0 ± 0.5	−6.9 ± 0.5
10	19.8	1.8	−3.8 ± 0.4	−3.9 ± 0.4	−6.6 ± 0.4
20	16.5	1.4	−3.6 ± 0.3	−3.7 ± 0.3	−6.3 ± 0.3
50	12.0	0.9	−3.6 ± 0.2	−3.1 ± 0.2	−5.2 ± 0.2
100	8.9	0.6	−3.5 ± 0.1	−2.9 ± 0.1	−4.65 ± 0.1
175	6.9	0.4	-	-	−4.3 ± 0.1
250	5.8	0.3	−3.5 ± 0.1	−3.12 ± 0.1	-

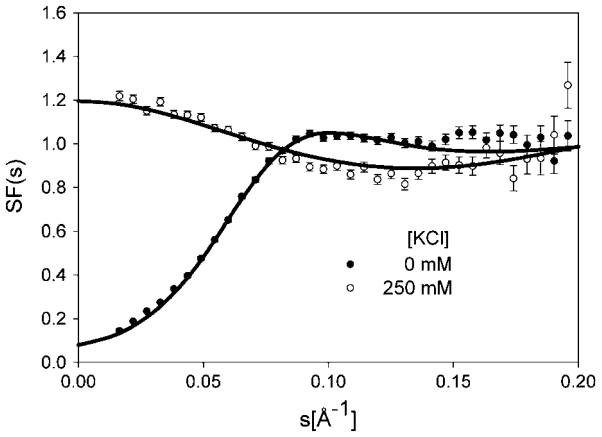

FIGURE 3 Experimental and calculated (*thick line*) structure factor with statistical errors for a lysozyme solution (68 mg/ml) in 0 mM and 250 mM KCl in water. For clarity only 1 experimental point in 20 is displayed. Note the systematic deviations, especially in the attractive regime (250 mM KCl).

6 and a value of σ of 34.4 Å. In the range 0–50 mM KCl, the average χ^2 ($\chi^2 = \sum_k (I_{calc} - I_{obs})^2 / I_{obs}$) calculated for 13 data points ($k = 13$) in the range $0.016 < s < 0.2$ Å^{-1} is 0.025 independent of the type of potential—fixed or variable—used. The values at 100 and 250 mM KCl are, however, significantly higher (0.07 and 0.20 for the fixed potential against 0.03 and 0.10 for the variable potential).

Values in the same range ($d_a = 3$ Å, $J_a = -2.65$ kT) but with a particle diameter of 32.4 Å were found for a similar NaCl (0–350 mM) concentration series at 100 mg/ml lysozyme at pH 4.5 (6). In this study, the number of charges needed to fit the data slowly decreased from 6 at 0 mM NaCl to 5.1 at 210 mM NaCl and then abruptly dropped to 2.9 at 280 mM NaCl, which is difficult to explain by screening effects but probably corresponds to the onset of aggregation. This is also suggested by the results of hydrogen titration of lysozyme in KCl solutions yielding a charge of 11 at pH 4.5, which decreases by at most one unit in the range of ionic strength between 0.1 and 2 M (23). The possibility that a higher salt concentration may lead to stronger attraction as predicted by theoretical considerations (24) while simultaneously reducing repulsion through screening was previously considered in the interpretation of the influence of pH and temperature on the structure factor (6). In our calculations, the depth of the attractive potential decreases with increasing salt concentration, but this effect is more than offset by the reduction of the depth of the repulsive potential resulting from the decreasing Debye length.

Clearly, the calculation of structure factors is not unique and the main justification for preferring a variable attractive potential in this study is given by the analysis of the results for the lysozyme solutions containing TMAO. Whereas the structure factor in the absence of salt is similar in 250 mM urea and in water as illustrated in Fig. 4, the curve in 250 mM TMAO differs significantly. The difference is even more pronounced in the attractive regime where the TMAO sample with 250 mM KCl is precipitated. The strong influence of TMAO on the structure factor is confirmed by the results for a TMAO concentration series (0–1 M) in absence of salt in Fig. 5. It is not possible to account for the structure factors for the KCl concentration series in 250 mM TMAO in Fig. 6

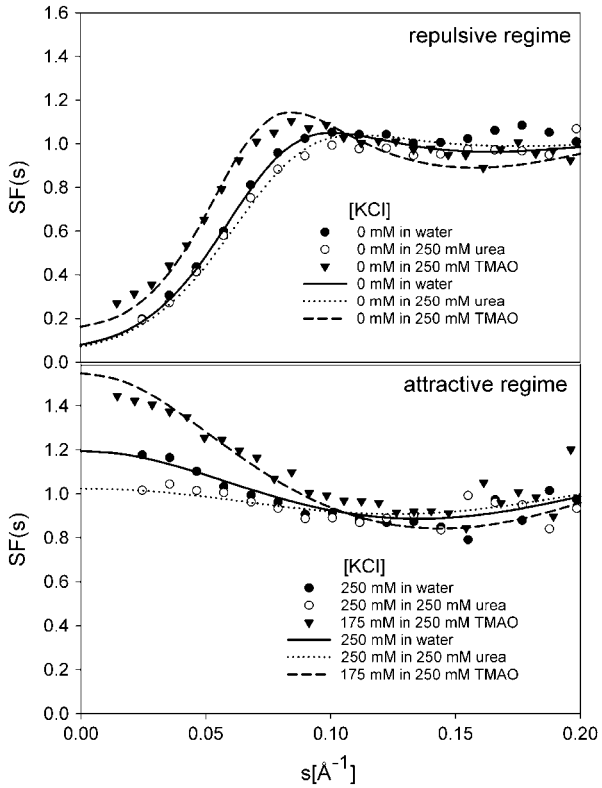

FIGURE 4 Experimental (*symbols*) and calculated structure factors for a lysozyme solution (68 mg/ml) in absence of salt in water, 250 mM urea, or 250 mM TMAO (*top*) and in solutions with 250 mM KCl or 250 mM KCl and 250 mM urea or 175 mM KCl and 250 mM TMAO (*bottom*).

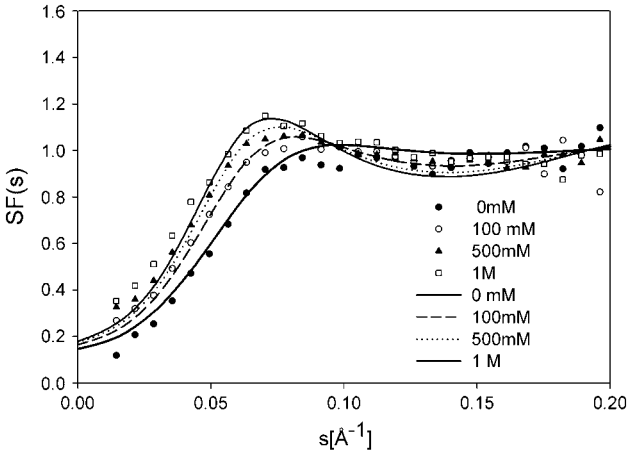

FIGURE 5 Experimental (*symbols*) and calculated structure factors of a lysozyme (45.5 mg/ml) solution in deionized water at TMAO concentrations between 0 and 1 M. The values of J_a used for the fits are 0 mM, −5.3 kT; 100 mM, −7.5 kT; 500 mM, −7.9 kT; and 1 M, −7.9 kT.

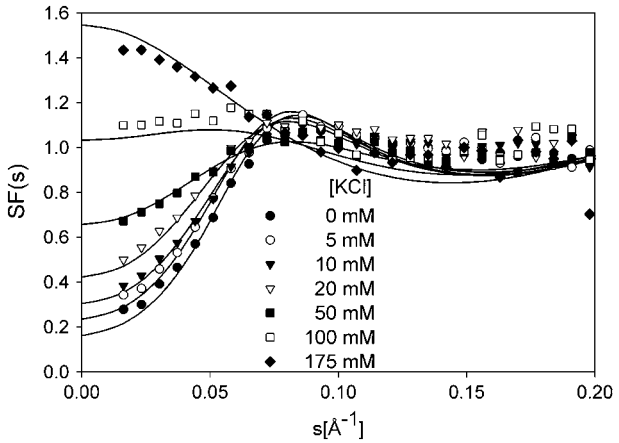

FIGURE 6 Experimental and calculated (*thick lines*) structure factors for a KCl concentration series in a lysozyme solution (68 mg/ml) containing 250 mM TMAO. Note that the attractive interactions are significantly higher than for the corresponding KCl concentration series in Fig. 2.

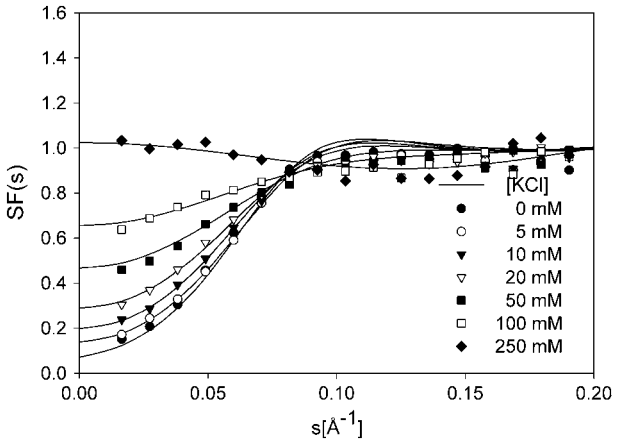

FIGURE 7 Experimental and calculated (*thick lines*) structure factors for a KCl concentration series in a lysozyme solution (68 mg/ml) containing 250 mM urea. The hard sphere radius, effective charge, Debye length, and range of the attractive potential in the calculations were the same as for the measurements in deionized water.

with a variable repulsive potential. Although, the data in absence of salt can be described using a stronger attractive potential than for the solutions in deionized water or urea, if one assumes that this value remains constant for the entire salt series the onset of the calculated structure factors in the attractive regime is much larger than the experimental one. This onset is very sensitive to variations in the depth of the attractive potential in the attractive regime, whereas in the repulsive regime it hardly changes with only minor differences in the range $0.07\ \text{Å}^{-1} < s < 0.20\ \text{Å}^{-1}$. The higher uncertainty in the J_a values in the repulsive regime (at low salt concentrations) is also reflected in the errors in Table 1.

The possibility that the difference between the structure factors in water and 250 mM TMAO would be due to dimer formation at higher protein concentration can be excluded. Indeed, analyses of the form factor at low protein concentration in 250 mM TMAO give the same result as in water and correspond to monomers as shown in Fig. 1. If there had been extensive dimerization, the average level of the structure factor would have been significantly above one in the range $s < 0.15\ \text{Å}^{-1}$, which was observed neither in the series with increasing TMAO concentrations in Fig. 5 nor in the KCl concentration series in 250 mM TMAO in the repulsive regime in Fig. 6.

The same repulsive potential can be used to describe the electrostatic interactions between the lysozyme molecules with the different cosolutes used here. This is illustrated in Fig. 7 for the KCl concentration series in 250 mM urea. The values for the depth of the attractive potential corresponding to the results in deionized water, 250 mM TMAO, and 250 mM urea are given in Table 1. The differences between the parameters for the salt series in deionized water and in 250 mM urea reflect a weaker attractive potential in the presence of urea: J_a between -3.7 and -3.12 compared to -5.3 and -3.5 kT at 20°C for deionized water.

In contrast, the parameters for the series in 250 mM TMAO structure reveal a significant increase in the attractive potential compared to the situation in deionized water or 250 mM urea. With the same values for the parameters defining the repulsive potentials and the range of the attractive potential, a depth between -6.9 and -4.3 kT at 20°C is obtained. This result is in agreement with the observation that TMAO counteracts the effect of urea (8) mainly by altering the balance between preferential binding of urea and preferential exclusion of TMAO, corresponding to increased hydration (25). Molecular dynamics calculations also suggest that neither urea nor TMAO make direct interactions, which would significantly affect the effective charge of the protein at the relatively low concentrations used here and imply that the cosolutes mainly affect the structure and dynamics of water (26), which are likely to be reflected by the parameters of the attractive potential.

CONCLUSION

The results confirm that the structure factors for a KCl concentration series (0–250 mM) at a fixed lysozyme concentration (68 mg/ml) can be well represented by assuming a fixed attractive potential and a variable effective charge as shown by others (6). Attempts to extend this approach to the modeling of the structure factors of lysozyme solutions in the presence of 250 mM TMAO and KCl indicate that the experimental observations can only be explained using a variable attractive potential and a constant effective charge. For this reason, the data for the KCl concentration series on lysozyme in distilled water and 250 mM urea were reanalyzed and a better agreement was also found. This does not exclude the possibility that in other circumstances (e.g., a pH series) the use of a variable effective charge could not

be preferable, but suggests that the two options should be carefully considered. In some cases the choice may be facilitated by independent measurements of the charge of the protein by hydrogen titration (23) or capillary electrophoresis (27), even if this is only indirectly related to the effective charge.

Finally, it should be noted that Eq. 1 is only strictly valid in the repulsive regime since in the attractive regime formation of oligomers results in polydispersity. In a solution of monodisperse aggregates (e.g., dimers or other 1:1 complexes), the structure factor contains, however, useful structural information allowing one to deduce the relative arrangement of the monomers (see, e.g., Moore and Engelman (28)). How easily this information can also be extracted from mixtures of known composition remains a matter for further investigation. At this stage it should also be considered whether the balance between preferential binding and/or preferential exclusion (or preferential hydration) of cosolutes may not be more effectively investigated by neutron scattering, which offers more possibilities of varying the contrast than x-ray scattering.

M.N. thanks Prof. Dr. Robert L. Johnson for his interest in the work and his encouragement, and Maxim Petoukhov, Anni Linden, Katja Schirwitz, and Will Stanley for their help.

REFERENCES

1. Israelachvili, J. 1992. Intermolecular & Surface Forces. Academic Press, London.
2. Hochachka, P. W., and G. N. Somero. 2002. Biochemical Adaptation. Oxford University Press, New York.
3. Bloemendal, H., W. de Jong, R. Jaenicke, N. H. Lubsen, C. Slingsby, and A. Tardieu. 2004. Ageing and vision: structure, stability and function of lens crystallins. *Prog. Biophys. Mol. Biol.* 86:407–485.
4. Koch, M. H. J., P. Vachette, and D. I. Svergun. 2003. Small-angle scattering: a view on the properties, structures and structural changes of biological macromolecules in solution. *Q. Rev. Biophys.* 36:147–227.
5. Malfois, M., F. Bonneté, L. Belloni, and A. Tardieu. 1996. A model of attractive interactions to account for fluid-fluid phase separation of protein solutions. *J. Chem. Phys.* 105:3290–3300.
6. Tardieu, A., A. Le Verge, M. Malfois, F. Bonneté, S. Finet, M. Riès-Kautt, and L. Belloni. 1999. Proteins in solution: from x-ray scattering intensities to interaction potentials. *J. Cryst. Growth.* 196:193–203.
7. Finet, S., D. Vivarés, F. Bonneté, and A. Tardieu. 2003. Controlling biomolecular crystallization by understanding the distinct effects of PEGs and salts on solubility. *Methods Enzymol.* 368:105–129.
8. Lin, T. Y., and S. N. Timasheff. 1994. Why do some organisms use a urea-methylamine mixture as osmolyte? Thermodynamic compensation of urea and trimethylamine N-oxide interactions with protein. *Biochemistry.* 33:12695–12701.
9. Bennion, B. J., and V. Daggett. 2003. The molecular basis for the chemical denaturation of protein by urea. *Proc. Natl. Acad. Sci. USA.* 100:5142–5147.
10. Bennion, B. J., and V. Daggett. 2004. Counteraction of urea-induced protein denaturation by trimethylamine N-oxide: a chemical chaperone at atomic resolution. *Proc. Natl. Acad. Sci. USA.* 101:6433–6438.
11. Koch, M. H. J., and J. Bordas. 1983. X-ray diffraction and scattering of disordered systems using synchrotron radiation. *Nuclear Instrum. Methods.* 208:461–469.
12. Gabriel, A. 1977. Position sensitive x-ray detector. *Rev. Sci. Instrum.* 48:1303–1305.
13. Konarev, P. V., V. V. Volkov, A. V. Sokolova, M. H. J. Koch, and D. I. Svergun. 2003. PRIMUS: a Windows PC-based system for small-angle scattering data analysis. *J. Appl. Crystallogr.* 36:1277–1282.
14. Svergun, D. I. 1992. Determination of the regularization parameter in indirect-transform methods using perceptual criteria. *J. Appl. Crystallogr.* 25:495–503.
15. Verwey, E. J. W., and J. T. G. Overbeek. 1948. Theory of the Stability of Lyophobic Colloids. Dover Publications, Mineola, NY.
16. Kaatze, U., H. Gerke, and R. Pottel. 1986. Dielectric relaxation in aqueous solutions of urea and some of its derivatives. *J. Phys. Chem.* 90:5464–5469.
17. Shikata, T., and S. Itatani. 2002. Dielectric relaxation of aqueous trimethylamineoxide solutions. *J. Solut. Chem.* 31:823–844.
18. Belloni, L. 1993. Inability of the hypernetted chain integral equation to exhibit a spinodal line. *J. Chem. Phys.* 98:8080–8095.
19. Svergun, D. I., S. Richard, M. H. J. Koch, Z. Sayers, S. Kuprin, and G. Zaccai. 1998. Protein hydration in solution: experimental observation by x-ray and neutron scattering. *Proc. Natl. Acad. Sci. USA.* 95:2267–2272.
20. Vaney, M. C., S. Maignan, M. Riès-Kautt, and A. Ducruix. 1996. High-resolution structure (1.33Å) of a HEW lysozyme tetragonal crystal grown in the APCF apparatus. Data and structural comparison with a crystal grown under microgravity from SpaceHab-01 mission. *Acta Crystallogr.* D52:505–517.
21. Berman, H. M., J. Westbrook, Z. Feng, G. Gilliland, T. N. Bhat, H. Weissig, I. N. Shindyalov, and P. E. Bourne. 2000. The Protein Data Bank. *Nucleic Acids Res.* 28:235–242.
22. Svergun, D. I., C. Barberato, and M. H. J. Koch. 1995. CRYSOL—a program to evaluate x-ray solution scattering of biological macromolecules from atomic coordinates. *J. Appl. Crystallogr.* 28:768–773.
23. Kuehner, D. E., J. Engmann, F. Fergg, M. Wernick, H. W. Blanch, and J. M. Prausnitz. 1999. Lysozyme net charge and in binding in concentrated aqueous electrolyte solutions. *J. Phys. Chem. B.* 103: 1368–1374.
24. Belloni, L., and O. Spalla. 1997. Attraction of electrostatic origin between colloids. *J. Chem. Phys.* 107:465–480.
25. Kita, Y., T. Arakawa, T.-Y. Lin, and S. N. Timasheff. 1994. Contribution of the surface free energy perturbation to protein-solvent interactions. *Biochemistry.* 33:15178–15189.
26. Zou, Q., B. J. Bennion, V. Daggett, and K. P. Murphy. 2002. The molecular mechanism of stabilization of proteins by TMAO and its ability to counteract the effects of urea. *J. Am. Chem. Soc.* 124:1192–1202.
27. Carbeck, J. D., I. J. Colton, J. R. Anderson, J. M. Deutch, and G. M. Whitesides. 1999. Correlations between the charge of proteins and the number of ionizable groups they incorporate: studies using protein charge ladders, capillary electrophoresis and Debye-Hueckel theory. *J. Am. Chem. Soc.* 121:10671–10679.
28. Moore, P. B., and D. M. Engelman. 1977. Model calculations of protein pair interference functions. *J. Mol. Biol.* 112:228–234.